Consequences of End-Group Fidelity for the Quantitative Analysis of Surface Grafting of Polymers

Supporting Information

Christian Rossner*

Leibniz-Institut für Polymerforschung Dresden e.V., Institut für Physikalische Chemie und Physik der Polymere, Hohe Straße 6, D-01069 Dresden, Germany.

*(C.R.) E-mail: rossner@ipfdd.de.

Table of contents

1. Kinetic model used for the performed PREDICI simulations

Initiation.

I_2	→	2 I	k_d, f
I + M	→	P(1)	k_i
R + M	→	Q(1)	k_i

Propagation.

P(s) + M	→	P(s+1)	k_p
Q(s) + M	→	Q(s+1)	k_p

RAFT pre-equilibria.

P(s) + RAFT-R	→	P-RAFT-R(s)	$k_{add(pre)}$
P-RAFT(s) + R	→	P-RAFT-R(s)	$k_{add(pre)}$
P-RAFT-R(s)	→	P(s) + RAFT-R	k_b
P-RAFT-R(s)	→	P-RAFT(s) + R	k_b
Q(s) + RAFT-R	→	Q-RAFT-R(s)	$k_{add(pre)}$
Q-RAFT(s) + R	→	Q-RAFT-R(s)	$k_{add(pre)}$
Q-RAFT-R(s)	→	Q(s) + RAFT-R	k_b
Q-RAFT-R(s)	→	Q-RAFT(s) + R	k_b

RAFT main-equilibria.

P-RAFT(s) + P(r)	→	P-RAFT-P(s) + P-RAFT-P(r)	$k_{add(main)}$
P-RAFT-P(s)	→	P-RAFT(s)	$k_b/2$
P-RAFT-P(s)	→	P(s)	$k_b/2$
Q-RAFT(s) + Q(r)	→	Q-RAFT-Q(s) + Q-RAFT-Q(r)	$k_{add(main)}$
Q-RAFT-Q(s)	→	Q-RAFT(s)	$k_b/2$
Q-RAFT-Q(s)	→	Q(s)	$k_b/2$
P-RAFT(s) + Q(r)	→	P-RAFT-Q(s) + Q-RAFT-P(r)	$k_{add(main)}$
Q-RAFT(s) + P(r)	→	Q-RAFT-P(s) + P-RAFT-Q(r)	$k_{add(main)}$
P-RAFT-Q(s)	→	P-RAFT(s)	$k_b/2$
P-RAFT-Q(s)	→	P(s)	$k_b/2$
Q-RAFT-P(s)	→	Q-RAFT(s)	$k_b/2$
Q-RAFT-P(s)	→	Q(s)	$k_b/2$

Termination.

P(s) + P(r)	→	T(s) + T(r)	k_t
Q(s) + Q(r)	→	U(s) + U(r)	k_t
P(s) + Q(r)	→	T(s) + U(r)	k_t

In this scheme, P-RAFT(s) and T(s) represent dormant and terminated thermal-initiator derived α-functional polymeric species of chain length s; Q-RAFT(s) and U(s) represent the dormant and terminated RAFT-agent derived α-end-functional polymeric species of chain length s. The main equilibria are modelled using two fictive polymeric species produced with $k_{add(main)}$ that act as chain length memory.[1] Because of the thereby invoked duplication of the unimolecular fragmentation step, $k_b/2$ is used as fragmentation rate coefficient for the main equilibria.[1]

Chain-length dependent termination was accounted for according to the composite model:[2]

$$k_t^{i,i} = \begin{cases} k_t^{1,1} \times i^{-\alpha_S} & \text{for } i \leq i_C \\ k_t^{1,1} \times {i_C}^{(\alpha_L - \alpha_S)} \times i^{-\alpha_L} & \text{for } i > i_C \end{cases}$$

With the cross-termination rate coefficients taken as geometric mean values:

$$k_t^{i,j} = \left(k_t^i k_t^j\right)^{0.5}$$

Chain-length dependent addition of macro-radicals to dormant species was accounted for as such:[3]

$$k_{add}^{i,j} = \left(\frac{1}{k_{add}^0} + \frac{1}{k_t^{1,1}} + \frac{1}{k_t^{i,j}}\right)^{-1}$$

Table S1 list the rate coefficients used in the performed PREDICI simulations.

Table S1. Parameter list as used for the simulations performed in this work.

parameter	value
k_d	1.1×10^{-4} s^{-1} [4]
k_i	10^4 $Lmol^{-1}s^{-1}$ [5]
k_p	1.3×10^3 $Lmol^{-1}s^{-1}$ [6]
$k_{add(pre)}^0$	4.0×10^4 $Lmol^{-1}s^{-1}$ [a]
$k_{add(main)}^0$	3.6×10^5 $Lmol^{-1}s^{-1}$ [b]
k_b	10^2 s^{-1} [5]
$k_t^{1,1}$	1.2×10^9 $Lmol^{-1}s^{-1}$ [7]
i_C	100 [7]
α_S	0.65 [7]
α_L	0.15 [7]

[a]calculated according to: $k_{add(pre)}^0 = (C_{tr(pre)}^0 \times k_p)/\phi$, with $C_{tr(pre)}^0 = 15.2$,[7] and assuming a partition coefficient $\phi = 0.5$; [b]calculated according to: $k_{add(main)}^0 = (C_{tr(main)}^0 \times k_p)/\phi$, with $C_{tr(main)}^0 = 140$ (value for 60 °C),[8] and assuming a partition coefficient $\phi = 0.5$.

2. Additional simulation results

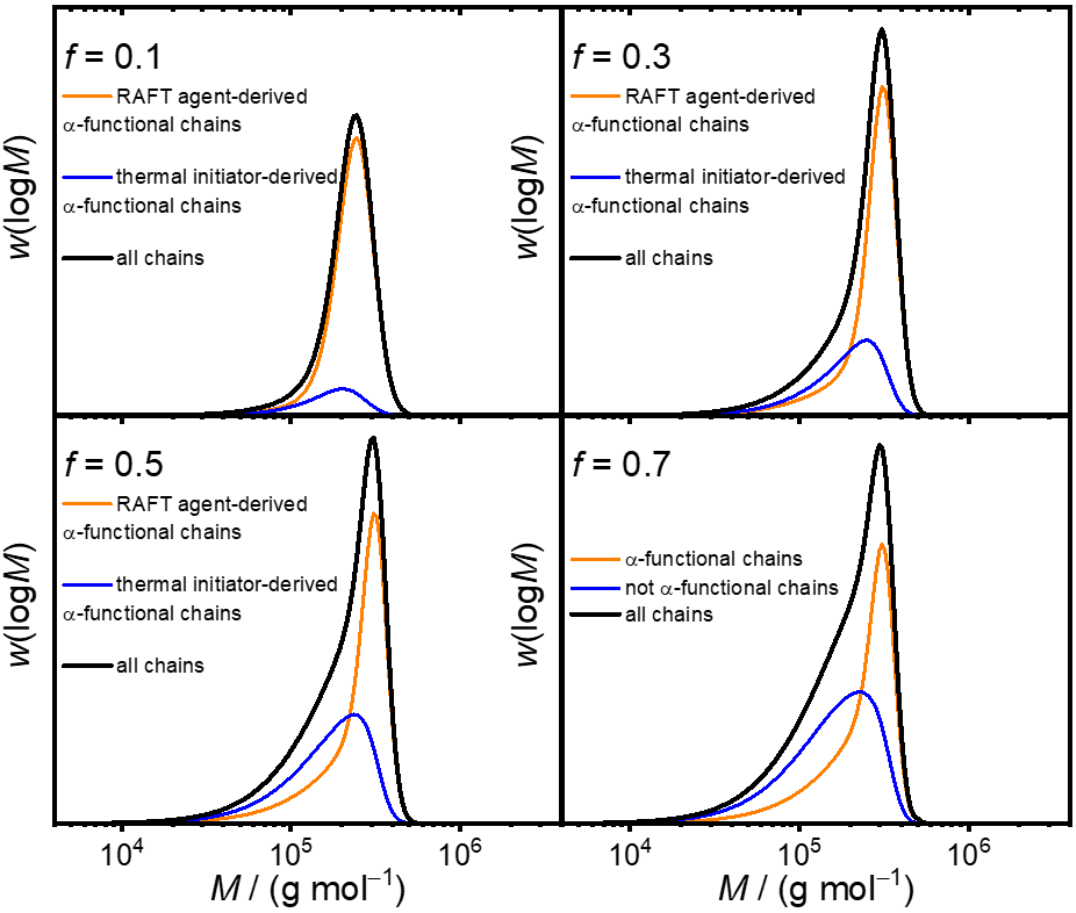

Figure S1. Simulated MMDs for RAFT-agent derived α-end-functional (orange) and thermal-initiator derived α-end-functional macromolecular species (blue). The overall MMD is shown in black. In the different panels initiator efficiency *f* is varied.

Table S2. Number-average (M_n) and weight-average molar masses (M_w) as well as dispersity values $Đ$ for RAFT-agent derived α-end-functional polymeric species, thermal-initiator derived α-end-functional polymeric species, and the overall polymeric material for different initiator efficiencies f.

$f = 0.1$			
Species	M_n / (g mol^{-1})	M_w / (g mol^{-1})	$Đ$
α-functional	$2.002 \cdot 10^5$	$2.347 \cdot 10^5$	**1.17**
Not α-functional	$1.343 \cdot 10^5$	$1.786 \cdot 10^5$	**1.33**
All chains	$1.884 \cdot 10^5$	$2.275 \cdot 10^5$	**1.21**

$f = 0.3$			
Species	M_n / (g mol^{-1})	M_w / (g mol^{-1})	$Đ$
α-functional	$2.174 \cdot 10^5$	$2.805 \cdot 10^5$	**1.29**
Not α-functional	$1.410 \cdot 10^5$	$2.010 \cdot 10^5$	**1.43**
All chains	$1.872 \cdot 10^5$	$2.568 \cdot 10^5$	**1.37**

$f = 0.5$			
Species	M_n / (g mol^{-1})	M_w / (g mol^{-1})	$Đ$
α-functional	$1.879 \cdot 10^5$	$2.615 \cdot 10^5$	**1.39**
Not α-functional	$1.207 \cdot 10^5$	$1.823 \cdot 10^5$	**1.51**
All chains	$1.529 \cdot 10^5$	$2.290 \cdot 10^5$	**1.50**

$f = 0.7$			
Species	M_n / (g mol^{-1})	M_w / (g mol^{-1})	$Đ$
α-functional	$1.703 \cdot 10^5$	$2.471 \cdot 10^5$	**1.45**
Not α-functional	$1.098 \cdot 10^5$	$1.752 \cdot 10^5$	**1.60**
All chains	$1.339 \cdot 10^5$	$2.117 \cdot 10^5$	**1.58**

3. Surface grafting scenarios

For surface grafting, only RAFT-agent derived chains are considered. Initially, the simulated MMD of these chains is shifted by applying equation 1 of Michalek et al.:[9]

$$k = \left(\frac{M_n}{M_i}\right)^{n^*} \quad \text{(S1)}$$

The shifted MMD is then multiplied by a correction factor, which is chosen such as to ensure grafting of 50 % of the mass of the overall polymeric material (i.e. RAFT-agent derived as well as thermal-initiator derived) to the surface, as described in ref. 9 of this document.

Because of the tailing of the simulated MMDs of this work at lower molar masses, such procedure results in shifted MMDs (i.e. surface-grafted MMDs) in which below a certain molar mass more chains are present in the shifted distribution than in the initial distribution. This is exemplarily shown for the MMD of RAFT-agent derived α-functional chains obtained from simulations performed for f = 0.2 (as initial distribution). The initial shifted distribution is obtained as described above, applying n^* = 1.0 (see Figure S2, panel A, below).

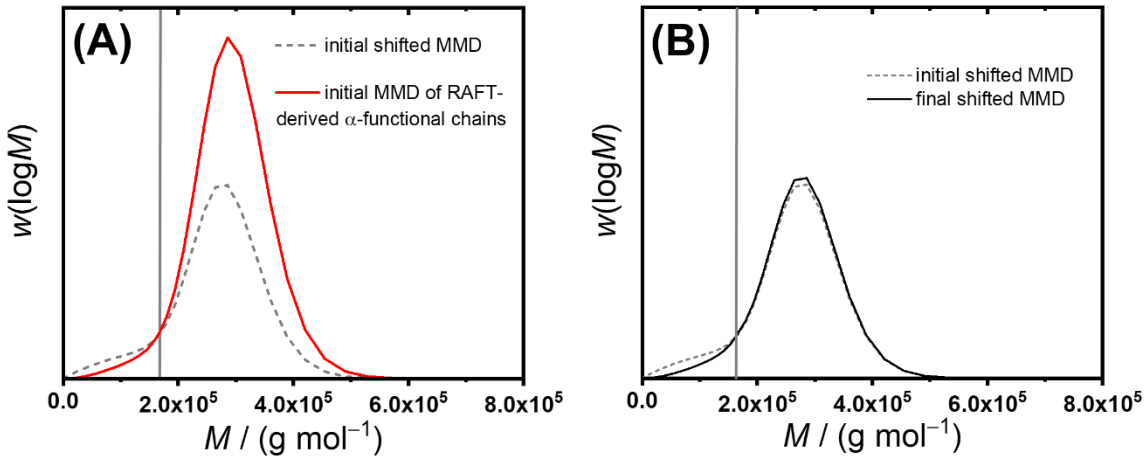

Figure S2. Panel A: Initial MMD of RAFT-agent derived α-functional chains obtained from simulations performed for f = 0.2 (red trace) and initially obtained shifted distribution (dashed grey trace). Non-physical values for the shifted distribution are obtained for molar masses below a certain threshold (indicated by the grey vetical line). Panel B: A shifted MMD without non-physical values (black trace) is obtained from the procedure described below.

To account for the appearance of non-physical values in parts of the shifted distribution, the following procedure was applied: Below the threshold molar mass, the shifted MMD was assumed to take the values of the start distribution (i.e. complete surface grafting) and above this threshold molar mass, the originally calculated values for the shifted MMD were assumed. Thus, the originally applied correction factor is no longer valid and a new correction factor needs to be applied, which may lead to the appearance of non-physical values in the shifted MMD again. These

steps are repeated iteratively, leading to decreasing correction factors in every new iteration step. Once the new correction factor is below 1 % (after few iterations), the procedure is stopped and the final shifted MMD is obtained (see Figure S2, panel B). The iterative procedure is summarized below:

Step 1: Calculate the shifted MMD according to equation S1.

Step 2: Apply a correction factor to the shifted MMD such that 50 % of the mass of the overall polymeric material are contained in the shifted MMD.

Step 3: Eliminate non-physical values in the MMD obtained from step 2.

Step 4: Repeat steps 2 and 3 until correction a factor < 1 % is obtained.

Surface grafting scenarios for simulated MMDs obtained for $f = 0.2$ and $n^* = 0.5$ as well as $n^* = 1.0$ in equation S1 are shown in Figure S3. From Figure S3 panel (C) it can be seen that M_w shifts between surface grafted species and all solution species of only 3 % and even -2 %, i.e. a higher M_w of the surface grafted species compared with all solution species, are obtained. This is not consistent with experimental observations in ref. 9 of this document. Consistency with the experimental observations in ref. 9 of this document is reached when $n^* = 1.4$ and $n^* = 4.0$ are used to calculate the MMD shift. These results are shown in Figure S2 in the main text.

A Surface grafting scenario for simulated MMDs obtained for $f = 0.1$ and $n^* = 1.0$ in equation S1 is shown in Figure S4. Here, due to the presence of less thermal-initiator derived chains, the normalized MMDs of surface-grafted and solution polymer species are more well behaved in the sense that a clear shift for the surface-grafted species to lower molar masses can be seen for both the low and high molar mass shoulder of the MMD (Figure S4, panel (A)). However, still, the presence of thermal-initiator derived chains manifests itself in different M_w shifts depending on whether all solution species or only solution species with RAFT-agent derived α-end groups are considered (Figure S4, panel (B)).

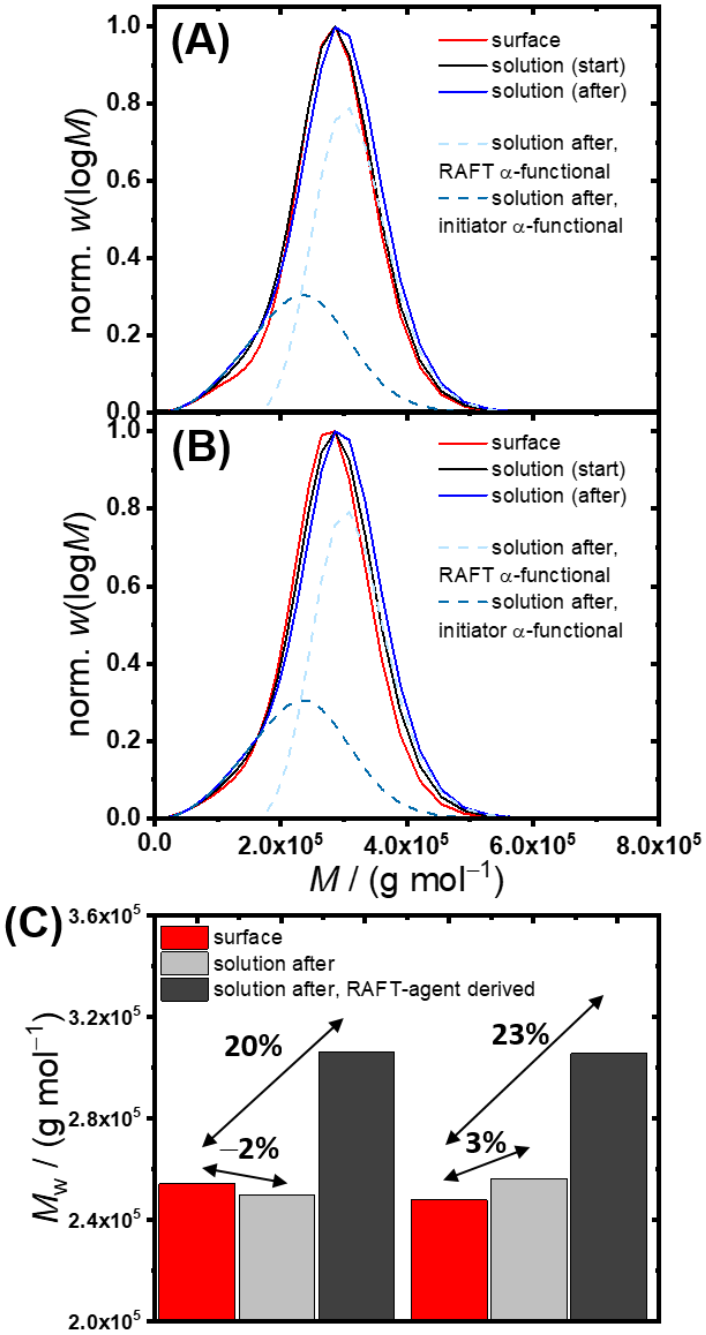

Figure S3. Polymer surface-grafting scenarios obtained by applying $n^* = 0.5$ (A) and $n^* = 1.0$ (B) in equation S1 to simulated MMDs obtained for $f = 0.2$. In panel (C), the M_w values for surface-grafted polymer species (red bars), all solution polymer species (light grey bars), and RAFT-agent derived α-end-functional solution polymer species (dark grey bars) as well as respective relative M_w shifts are displayed.

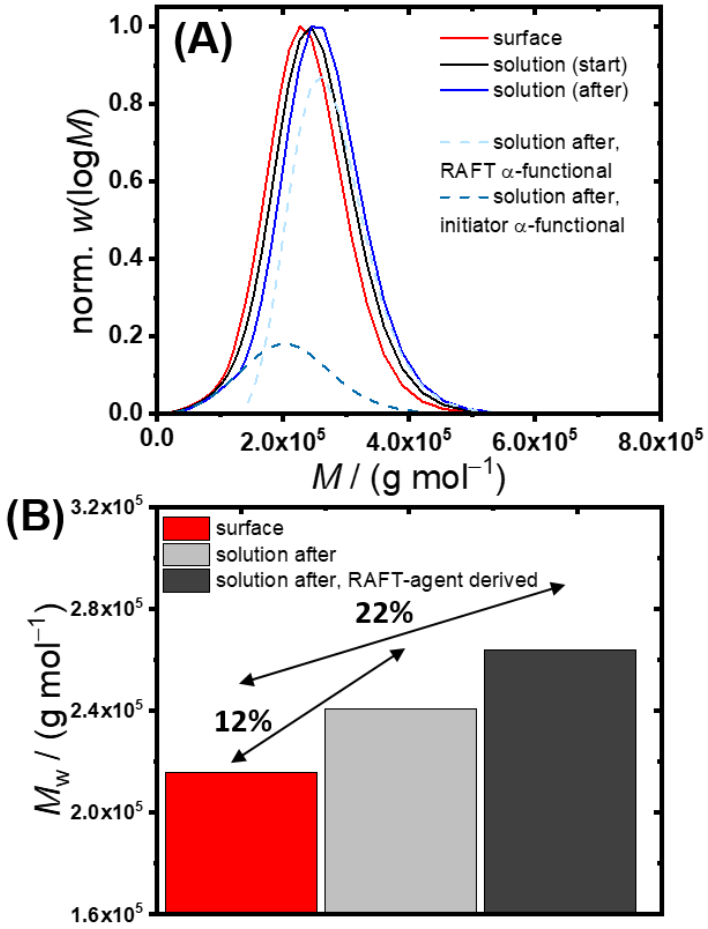

Figure S4. Polymer surface-grafting scenarios obtained by applying $n^* = 1.0$ (B) in equation S1 to simulated MMDs obtained for $f = 0.1$. In panel (B), the M_w values for surface-grafted polymer species (red bars), all solution polymer species (light grey bars), and RAFT-agent derived α-end-functional solution polymer species (dark grey bars) as well as respective relative M_w shifts are displayed.

Table S3. Number-average (M_n) and weight-average molar masses (M_w) as well as dispersity values $Đ$ for RAFT-agent derived α-end-functional polymeric species, thermal-initiator derived α-end-functional polymeric species, and the overall polymeric material for the two grafting scenarios discussed in the main text (Figure 2).

f = 0.2; n^* = 1.4 (Figure 2A in main text)			
Species	**M_n / (g mol^{-1})**	**M_w / (g mol^{-1})**	**$Đ$**
Surface	**$1.907 \cdot 10^5$**	**$2.447 \cdot 10^5$**	**1.28**
Solution (start)	**$1.957 \cdot 10^5$**	**$2.522 \cdot 10^5$**	**1.29**
Solution (after)	**$2.013 \cdot 10^5$**	**$2.599 \cdot 10^5$**	**1.21**
Solution after, RAFT-agent derived	**$3.035 \cdot 10^5$**	**$3.128 \cdot 10^5$**	**1.03**
Solution after, thermal-initiator derived	**$1.433 \cdot 10^5$**	**$1.964 \cdot 10^5$**	**1.37**

f = 0.2; n^* = 4.0 (Figure 2B in main text)			
Species	**M_n / (g mol^{-1})**	**M_w / (g mol^{-1})**	**$Đ$**
Surface	**$1.888 \cdot 10^5$**	**$2.366 \cdot 10^5$**	**1.25**
Solution (start)	**$1.957 \cdot 10^5$**	**$2.522 \cdot 10^5$**	**1.29**
Solution (after)	**$2.041 \cdot 10^5$**	**$2.696 \cdot 10^5$**	**1.32**
Solution after, RAFT-agent derived	**$3.284 \cdot 10^5$**	**$3.347 \cdot 10^5$**	**1.02**
Solution after, thermal-initiator derived	**$1.433 \cdot 10^5$**	**$1.964 \cdot 10^5$**	**1.37**

4. References

[1] P. Vana, T. P. Davis, C. Barner-Kowollik, *Macromol. Theory Simulations* **2002**, *11*, 823–835.

[2] G. B. Smith, G. T. Russell, J. P. A. Heuts, *Macromol. Theory Simulations* **2003**, *12*, 299–314.

[3] G. Johnston-Hall, M. J. Monteiro, *Macromolecules* **2007**, *40*, 7171–7179.

[4] A. Theis, A. Feldermann, N. Charton, M. H. Stenzel, T. P. Davis, C. Barner-Kowollik, *Macromolecules* **2005**, *38*, 2595–2605.

[5] P. B. Zetterlund, G. Gody, S. Perrier, *Macromol. Theory Simulations* **2014**, *23*, 331–339.

[6] S. Beuermann, M. Buback, T. P. Davis, R. G. Gilbert, R. A. Hutchinson, A. Kajiwara, B. Klumperman, G. T. Russell, J. Schweer, A. M. Van Herk, *Macromol. Chem. Phys.* **1997**, *198*, 1545–1560.

[7] G. Johnston-Hall, A. Theis, M. J. Monteiro, T. P. Davis, M. H. Stenzel, C. Barner-Kowollik, *Macromol. Chem. Phys.* **2005**, *206*, 2047–2053.

[8] A. Goto, K. Sato, Y. Tsujii, T. Fukuda, G. Moad, E. Rizzardo, S. H. Thang, *Macromolecules* **2001**, *34*, 402–408.

[9] L. Michalek, K. Mundsinger, L. Barner, C. Barner-Kowollik, *ACS Macro Lett.* **2019**, *8*, 800–805.